Biochimica et Biophysica Acta, 692 (1982) 431–440
Elsevier Biomedical Press

BBA 71437

UNIFORM IONOPHORE A23187 DISTRIBUTION AND CYTOPLASMIC CALCIUM BUFFERING IN INTACT HUMAN RED CELLS

LARS OLE SIMONSEN *, JØRGEN GOMME and VIRGILIO L. LEW

August Krogh Institute, University of Copenhagen (Denmark) and Physiological Laboratory, Cambridge University, Cambridge CB2 3EG (U.K.)

(Received June 30th, 1982)

Key words: Ionophore A23187; $^{45}Ca^{2+}$ flux; Ca^{2+} permeability; Cytoplasmic Ca buffering; (Human erythrocyte)

The divalent cation-selective ionophore A23187 has been used to characterize cytoplasmic Ca and Mg buffering, Ca^{2+}-pump parameters and the properties of a Ca^{2+}-activated K^+-channel in intact red cells. A critical assumption in these studies has been that the ionophore causes a uniform increase in divalent cation-permeability in all the cells. This has now been tested directly in ATP-depleted human red cells by analysing the kinetics of ionophore-induced ^{45}Ca-tracer and net Ca^{2+} fluxes. The experimental curves were all adequately fitted by single-exponentials at all ionophore concentrations tested. Moreover, statistical analysis of 61 individual tracer influx curves and of pooled data showed no trend towards fast second exponential components. These results demonstrate uniformity of ionophore distribution, ionophore-induced Ca^{2+}-permeability, and cytoplasmic Ca-buffering among all the cells. Experiments involving mixing of cell suspensions with high and low original ionophore content, and involving ionophore extraction by albumin, demonstrate a rapid redistribution of ionophore among the cells, indicating that homogeneity of ionophoric effects is achieved through dynamic ionophore redistribution.

Introduction

The divalent cation-selective ionophore A23187 is widely used as a tool to control the Ca^{2+} and Mg^{2+} permeability of biological membranes [1–4]. In red cells, analysis of the Ca and Mg redistribution after ionophore addition has led to the characterization of the cytoplasmic Ca and Mg buffering behaviour, Ca^{2+}-pump kinetics and properties of the Ca^{2+}-activated K^+-channel of intact cells [3–9]. The rapid onset of the Ca^{2+}- or Mg^{2+}-permeability change on addition of the ionophore to well-stirred cell suspensions, together with the fact that the original low permeability can be restored by washing the ionophore away [3,9–11], led to the assumption that ionophore contents and ionophoric effects become equal in all cells after brief initial transients [10]. This is an important point since many of the conclusions derived from the Ca and Mg distribution analysis depend on there being a uniform divalent cation permeability throughout the cell population. Hoffman et al. [12] have recently claimed heterogeneity of Ca^{2+}-permeability and content, and consequently of K^+-permeability, when low concentrations of ionophore (about 1 μM) are added to suspensions of fed red cells under conditions meant to reproduce those of Lew and Ferreira [9]. At high ionophore concentrations a nonuniform ionophore distribution would have much less effect because even low-ionophore cells would have a sufficiently

* Address for correspondence: Zoophysiological Laboratory B, August Krogh Institute, 13 Universitetsparken, DK-2100 Copenhagen Ø, Denmark.

Abbreviations: EGTA, ethylene glycol bis(β-aminoethyl ether)-*N,N,N',N'*-tetraacetic acid; Tris, tris(hydroxymethyl) aminomethane.

high Ca^{2+}-permeability to allow Ca-equilibration despite opposing Ca^{2+}-pump fluxes. The possibility that most of the ionophore added could become associated with only a minor fraction of the cells and hence contribute to create and maintain an uneven Ca distribution among the cells, particularly at the lower ionophore concentrations, was now investigated in detail.

In this paper we report experiments on $^{45}Ca^{2+}$-flux kinetics in ATP-depleted human red cells which demonstrate uniform ionophoric effects and cytoplasmic Ca-buffering behaviour. We also provide evidence that homogeneity of ionophore content is achieved through dynamic ionophore redistribution among the cells, and discuss the possible extent of Ca-content heterogeneity in fed red cells at low ionophore concentrations. A preliminary report of this study has been presented [13].

Materials and Methods

Principle of the method. Heterogeneity of red cell Ca content after ionophore addition could arise from differences in ionophore-induced Ca^{2+}-permeability, active Ca^{2+}-extrusion rate, or both. When the Ca^{2+}-pump is inhibited, as in the ATP-depleted red cells used for the present experiments [14,10], heterogeneity of ionophore-induced Ca^{2+}-permeability can be explored without interference from Ca^{2+}-pump fluxes. If a low concentration of ionophore is added to a suspension of ATP-depleted red cells in the presence of Ca, cells without or with little ionophore would contain less Ca or reach equilibrium slower than cells with a higher ionophore content. This should give a range of exponential components in any curve measuring tracer exchange or net Ca^{2+} movements. As the concentration of added ionophore is increased, the fraction of cells without any ionophore should decrease and the measured overall Ca distribution level should become independent of the ionophore concentration, as now all the cells reach Ca equilibrium. Investigation of net or ^{45}Ca-tracer exchange Ca^{2+} fluxes and Ca distribution levels at various ionophore concentrations should therefore provide information on whether or not the ionophore-induced Ca^{2+}-permeability is heterogeneous.

Experimental protocol. The usual experimental protocol was as follows: red cells from fresh, heparinized blood were washed three times and resuspended in a solution containing (mM): KCl, 75; NaCl, 75; Tris-HCl (pH 7.4 at 37°C), 10, (solution A), and EGTA, 0.1. After addition of inosine (10 mM) and iodoacetamide (6 mM), the cell suspension (haematocrit ~ 10%) was incubated for 3 h at 37°C. This procedure is known to reduce the ATP levels to about 1 μmol/l cells [10,14]. After depletion, the cells were washed twice in solution A and twice more in the final suspension medium which contained, in addition, 0.1 mM $CaCl_2$ and 0.15 mM $MgCl_2$. In this solution, K^+ and Mg^{2+} are close to electrochemical equilibrium across the cell membrane and, after ionophore A23187 addition, the red cells maintain a constant volume, ionic composition and membrane potential despite large permeability changes to Mg^{2+}, Ca^{2+} and K^+ [3–5,7,8]. All the experiments reported in this paper were performed using red cells from the same donor.

The usual procedure for tracer influx measurements at Ca equilibrium was to start incubation (haematocrit ~ 10%) at 37°C and, after 5–10 min, add the required volume of a concentrated ionophore solution in absolute ethanol (2 mM) to give the final concentrations shown in the figures. After 5–60 min, to allow for Ca equilibration at the various ionophore concentrations, 1 μCi/ml of $^{45}Ca^{2+}$ (effectively carrier-free) was added to the cell suspension under vigorous magnetic stirring. 0.1 ml samples were taken at adequate time intervals and processed as reported before [3,5] to determine the ^{45}Ca content of the cells and cell suspensions.

Net Ca^{2+}-influx measurements were performed in a similar way except that the cells were initially resuspended in a Ca^{2+}-free medium containing 10 μM EGTA and the influx measurement was started with the addition of $^{45}CaCl_2$, to a final concentration of 0.1 mM, about 5 min after ionophore addition.

^{45}Ca-tracer efflux was measured after tracer equilibration had been attained by diluting 20-fold the external ^{45}Ca specific activity at a constant external concentration of Ca^{2+}. This was achieved by adding concentrated, pH-adjusted, equimolar Ca-EGTA to a final concentration of 2 mM. For net Ca^{2+} efflux measurements, excess neutralized

EGTA was added to the medium after ^{45}Ca equilibration to reduce external Ca^{2+} to below 10^{-7} M. Enough NaOH was added together with EGTA to prevent pH changes due to H^+ displacement by Ca^{2+} binding to EGTA.

In some of the experiments the ionophore concentration was buffered with the use of albumin in the 10–20 μM range, as described before [15–17]. When albumin was added in order to extract the ionophore from the cells, as in the experiment of Fig. 3, the final concentration used was 200 μM. Cell associated ionophore was measured as previously reported [15].

Materials. The ionophore A23187 was a gift from Lilly Research Laboratories in the U.K. The albumin used was Sigma (London) crystallized and lyophilized (Cat. reference A 4378). For the experiment of Fig. 3 defatted albumin was used (Sigma Cat. reference A 7511). All reagents were analytical grade.

Calculations of Ca-content and Ca^{2+}-flux parameters. The Ca content of the cells at equilibrium (Ca_i^T) was determined from the measured total (A_T) and cell associated ^{45}Ca after tracer equilibration (A_i^∞), the haematocrit (H), and the known total Ca concentration in the cell suspension (Ca_T)

$$Ca_i^T = (A_i^\infty / A_T)(1/H)Ca_T.$$

This is justified because intact red cells are virtually Ca-free and there is no significant dilution of the external ^{45}Ca specific activity due to intracellular Ca-pools [18,19]. The fraction of ionized Ca within the cells, α, was calculated from the relation [3,5] $\alpha = r^2[Ca^{2+}]_o/Ca_i^T$, where r is the chloride distribution ratio, and $[Ca^{2+}]_o$ and Ca_i^T are the external ionized Ca concentration and internal total Ca content of the cells, respectively, at equilibrium. Under the experimental conditions used here $r^2 = 2.3$, corresponding to a membrane potential of -11 mV.

^{45}Ca-tracer and net influx curves were represented by equations of the form

$$A_i' = A_i^\infty(1 - \exp(-\lambda t)).$$

^{45}Ca-tracer efflux was analysed by

$$A_i' = A_i^\infty + (A_i^0 - A_i^\infty)\exp(-\lambda t),$$

and net efflux by

$$A_i' = A_i^0 \exp(-kt)$$

where A_i', A_i^0 and A_i^∞ are measured cell-associated ^{45}Ca activities at times t, zero and infinite, respectively. The observed rate constant, λ, is related to k, the rate constant of cellular exchange or efflux, by the expression

$$\lambda = k\left(1 + (H/(1-H))\left(Ca_i^T/[Ca^{2+}]_o\right)\right)$$

A small correction for the residual cell associated (or trapped) ^{45}Ca-activity (less than 0.5% of initial ^{45}Ca content of the cells) was applied to the net efflux curves. Except for the statistical treatment described below, a simple single-exponential analysis with fixed origin was applied to the curves shown in Figs. 1–4.

Statistical analysis of the Ca^{2+}-flux curves. The fitting of single- or double-exponential models to the data was made by computer using a maximum likelihood method [20]. In the analysis aimed at defining the detection limit for a small, fast component in single curves or in pooled data (Table III), the data were generated by computer as the sum of two exponential terms plus a normally distributed stochastic component. In the generated data the number of points and the time values were taken from the corresponding experimental curves. The stochastic component was set equal to the scatter (defined as the square root of the residual mean of squares) of the experimental data as determined from the single-exponential fit with the origin fixed at 0.0. In the analysis of the individual curves of Table III both origin and asymptote were fixed. The approximate significance levels corresponding to differences between single and double exponential models were estimated from likelihood ratio tests using the variance ratio and the F-distribution [20].

Results

Ca^{2+} fluxes

Fig. 1 shows ^{45}Ca-tracer equilibration curves obtained at different ionophore concentrations in ATP-depleted red cells and Table I reports the relevant parameters. The figure is representative of

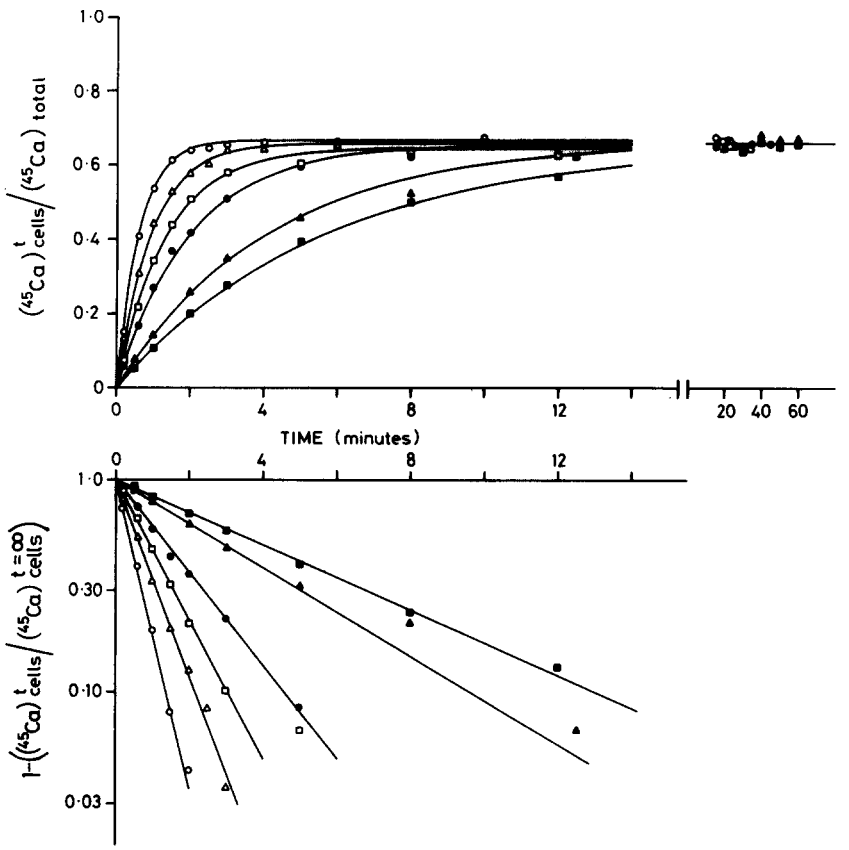

Fig. 1. Typical ^{45}Ca-tracer influx curves in Ca equilibrated, ATP-depleted red cells in the presence of ionophore A23187 (2.6–10 μmol/l cells). The curves were fitted by single exponentials with the origin fixed at 0.0 using a maximum likelihood programme. In the log plot (lower panel) the lines are drawn with a slope equal to the computed rate constants. The relevant parameters of the curves shown in the figure are given in Table I.

TABLE I

EXPERIMENTAL CONDITIONS AND RELEVANT PARAMETERS OF THE TYPICAL ^{45}Ca-TRACER INFLUX CURVES IN ATP-DEPLETED RED CELLS SHOWN IN FIG. 1

The curves were selected from the total of 61 ^{45}Ca-tracer influx curves analysed and arranged in order of increasing rate constants (and increasing cell ionophore content). $Ca_T = 88$ μmol/l cell suspension. For details of calculations of Ca content and Ca^{2+}-flux parameters see Methods. Alb, albumin.

Curve No.	Alb (μM)	Ionophore A 23187 added (μM)	Cell ionophore content (μmol/l cells)	A_i^{∞}/A_T	Ca_i^T (μmol/l cells)	$[Ca^{2+}]_o$ (μM)	α	λ (min^{-1})	k (h^{-1})
14	20	2.3	2.62	0.6516 ± 0.0031	527.0	34.4	0.149	0.1812 ± 0.0032	3.79
18	10	1.6	2.84	0.6608 ± 0.0069	534.5	33.5	0.143	0.2338 ± 0.0095	4.76
28	10	2.4	5.11	0.6511 ± 0.0039	526.6	34.5	0.149	0.5237 ± 0.0112	11.0
37	10	2.7	6.20	0.6428 ± 0.0066	519.9	35.3	0.155	0.7369 ± 0.0295	15.8
45	10	3.0	7.84	0.6588 ± 0.0026	532.9	33.7	0.144	1.069 ± 0.018	21.9
53	20	5.0	10.4	0.6666 ± 0.0026	539.2	32.9	0.139	1.589 ± 0.032	31.8

other experiments giving similar results and spanning a range of cell ionophore contents between 0.5 and 23 μmol/l cells, corresponding to ionophore concentrations (in the absence of albumin) between 0.1 and 5 μM. At all ionophore concentrations above 0.3 μM (2 μmol/l cells), the Ca_i^T at equilibrium was similar (535 ± 9.9 μmol/l cells (mean ± S.D.; 5 expts.)), indicating ionophore distribution within the whole cell population. The fraction of ionized Ca inside the cells (α) was calculated at 0.159 ± 0.013 (mean ± S.D.; 5 expts.). At all the ionophore concentrations tested, the tracer equilibration curves were adequately described by single-exponentials up to about 95% of the equilibrium value. At very low ionophore concentrations, down to 0.1 μM (0.5 μmol/l cells), the ^{45}Ca-tracer influx curves still followed single exponentials but the final internal Ca level was slightly reduced compared with that found at all ionophore concentrations above 0.3 μM (2 μmol/l cells). This may be due to some residual Ca^{2+}-pumping activity due to incomplete ATP-depletion, but the absence of ionophoric dimers from some cells cannot be ruled out. At ionophore concentrations above 2.5 μM (18 μmol/l cells) the fluxes were too fast to be monitored with the present technique.

Influx measurements are not very precise for estimating second exponential components near equilibrium levels, since one has to deal with small differences between large numbers. Net efflux curves following sudden reduction in external Ca^{2+} concentration are more likely to reveal the existence of small and slow exponential components as the Ca content of the cells is reduced. Fig. 2 shows the results of an experiment, representative of seven similar ones, with ionophore concentrations in the 0.3 to 2 μM range, in which the change in Ca content of the cells was followed after addition of excess EGTA. It can be seen that a single exponential describes the efflux kinetics down to 1% of the initial Ca content.

Similarly good single-exponential fits were observed in four net Ca influx experiments with ionophore concentrations in the 0.3 to 2 μM range and in a single ^{45}Ca-tracer efflux experiment at an ionophore concentration of 0.5 μM. The finding of single exponentials in net influx or efflux experiments also excludes generation of ionophore heterogeneity by sudden changes in external Ca^{2+} concentration or Ca^{2+}-gradients across the cell membrane.

Statistical analysis of the ^{45}Ca-tracer flux curves

The important question to be asked with the type of curves shown in Figs. 1 and 2 is at what level of significance, or with what degree of certainty, can the existence of multiple exponential components be ruled out, as required if the uniformity of ionophore-induced Ca^{2+}-permeability

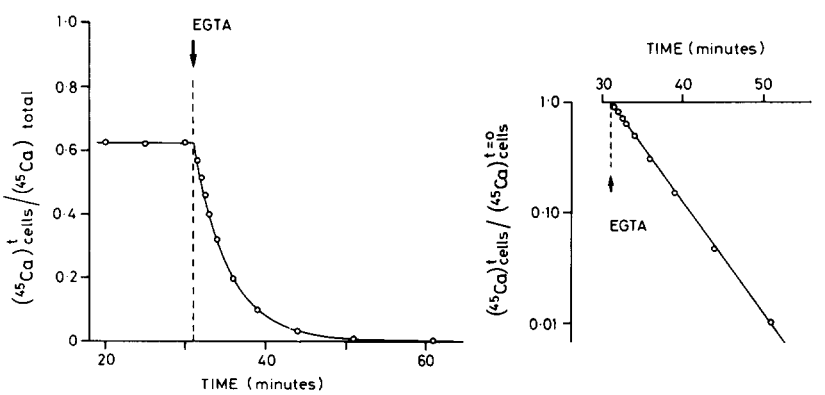

Fig. 2. Typical Ca^{2+} net efflux curve following addition of excess EGTA to ^{45}Ca-tracer equilibrated ATP-depleted red cells pre-incubated for 60 min in the presence of 0.5 μM ionophore A23187 (3.0 μmol/l cells). Ca_T = 90 μmol/l cell suspension. At Ca equilibrium Ca_i^T = 536 μmol/l cells, $[Ca^{2+}]_o$ = 37.8 μM; α = 0.161. The efflux was started by addition of 0.2 mM EGTA plus 0.2 mM NaOH. The rate constant was estimated at $k = 0.222 \pm 0.007$ min^{-1} (maximum likelihood estimate) and corresponds to the slope of the line given in the log plot.

in all the cells is to be demonstrated. The possibility [12] that only a few cells retain most of the ionophore makes it particularly relevant to estimate the degree of confidence with which the existence of small but fast exponential components can be ruled out.

We have analysed a total of 61 tracer influx curves, each having between 9 and 13 experimental points. The curves span a range of rate constants (λ) between 0.0227 and 3.74 min^{-1}, corresponding to measured mean cell ionophore contents in the range 0.5 to 18 μmol/l cells. Moreover, in order to increase the statistical sample, the data were pooled in groups after normalizing the rate constant and asymptote of each curve using the single-exponential fit with the origin fixed at 0.0. Pooling the data in this way should reinforce and help reveal any systematic trend away from single exponentiality, as in a signal averaging exercise. The experimental data were pooled in groups according to rate constants: (a) $\lambda < 0.20$ min^{-1} (15 curves, 168 points); (b) $0.40 < \lambda < 0.60$ min^{-1} (10 curves, 111 points), and (c) $\lambda > 1.0$ min^{-1} (18 curves, 202 points); finally, all the 681 points from the 61 normalized curves were pooled and analysed together.

Two types of statistical tests were performed. The first set of tests was aimed at evaluating whether a second exponential component could be demonstrated, at least in the low-ionophore curves. This was analysed by fitting single-exponential and double-exponential models to the data. The results showed that out of the 61 individual curves the double-exponential fit was significantly better ($P < 0.05$) than the single-exponential fit in only four curves. Furthermore, in these four cases the minor exponential component was slower than the main component. Three solutions produced by the maximum likelihood method indicated a small fast component, but in these three solutions the double-exponential fit was not significantly better than the single-exponential fit ($P = 0.19$, $P = 0.35$ and $P = 0.41$, respectively). The analysis of the pooled data is given in Table II. It can be seen that the maximum likelihood method produces double-exponential solutions only with a small and slow second component at all ionophore concentrations. The improvement over the single-exponential fit is only marginal in the low-ionophore (a) and 'all-data' groups ($P = 0.08$). The possible significance of the variation of the area to volume ratio in the cell population [21] for the slight deviation from single-exponential kinetics is currently under investigation.

Additional evidence for the lack of any trend towards a small fast component for all ionophore concentrations is provided by likelihood ratio analysis of the fits of single-exponential models

TABLE II

PARAMETERS OF THE DOUBLE-EXPONENTIAL MODEL AND APPROXIMATE SIGNIFICANCE OF DIFFERENCE WITH SINGLE-EXPONENTIAL MODEL AS DETERMINED BY CURVE FITTING (MAXIMUM LIKELIHOOD ESTIMATE) AND LIKELIHOOD RATIO TEST, RESPECTIVELY

Main compartment parameters in the double-exponential model remain close to unity and are omitted for simplicity. The compartment size and rate constant of the second exponential component should be compared with their normalized unity value in the single-exponential fit. Residual mean of squares, F (variance ratio) and P (probability) have the statistical meaning defined in Ref. 20.

Group	No. of curves	No. of data points	Second exponential component		Residual mean of squares $\times 10^{6}$ [a]	Likelihood ratio test	
			Fractional compartment size	Relative rate constant		F	P
Low ionophore (a)	15	168	0.062 ± 0.010	0.164 ± 0.144	53(66)	1.24	0.08
Medium ionophore (b)	10	111	0.060 ± 0.026	0.200 ± 0.114	208(250)	1.20	0.17
High ionophore (c)	18	202	0.016 ± 0.005	0.071 ± 0.065	170(179)	1.06	0.35
All data	61	681	0.038 ± 0.009	0.205 ± 0.059	148(165)	1.11	0.08

[a] The numbers in parenthesis give the residual mean of squares of the single-exponential fit.

with the origin fixed at 0.0 and with floating origin. In all 61 individual curves there was no significant difference between the fits of these two models, nor did pooling of the normalized experimental curves reveal any significant trend.

The second set of tests was intended to estimate the parameters of any small and fast exponential component that, with the precision of our measurements, might have become detectable at a significance level of $P \leq 0.05$. To improve the sensitivity of the test we used only data corresponding to the low ionophore concentrations because here the density of early experimental points is highest. The results in Table III show that in the individual curves, if there had been 5% of the cells with eight times or more the Ca^{2+}-permeability of the rest, this would have been detectable with $P \leq 0.05$. In the pooled data, a systematic trend in the individual curves would have rendered 5% of the cells with only 3.5 times the Ca^{2+}-permeability of the rest detectable with $P = 0.05$. This means that any component, fast enough to generate meaningful differences in ionophore-induced Ca^{2+}-permeability between a few cells and the rest, would have been easily detectable with the precision of our measurements. Moreover, any small fast component present in the experimental data must have been well below the detection limits discussed above since not even a trend towards a fast second exponential could be detected in the individual curves or in the pooled data. This means that any significant small, fast component can safely be excluded, even at ionophore concentrations far below the range for which heterogeneity of ionophore-induced Ca^{2+}-permeability has been claimed [12].

TABLE III

FRACTIONAL COMPARTMENT SIZE AND MINIMUM VALUE OF RATE CONSTANT OF FAST SECOND EXPONENTIAL COMPONENT OF COMPUTER-GENERATED DATA, REQUIRED FOR SIGNIFICANCE ($P \leq 0.05$) OF DIFFERENCE OF DOUBLE-EXPONENTIAL WITH SINGLE-EXPONENTIAL MODEL AT THREE FAST COMPARTMENT SIZES COMPRISING 20, 10 AND 5% OF THE CELLS

The five individual curves analysed correspond to rate constants in the 0.02 to 0.05 min^{-1} range. The pooled data are those of the low-ionophore group (a) of Table II. The stochastic component of the computer-generated data (see Methods) was, for the pooled data, set equal to the precision of the experimental measurements (0.8%), as calculated from the scatter of the experimental points around the single-exponential curve with fixed origin. The same value was used in the analysis of the five individual curves. The parameters were estimated using the maximum likelihood method and the significance evaluated by the likelihood ratio test.

Fractional compartment size	Minimum value of Relative rate constant for $P \leq 0.05$	
	Individual curves	Pooled data
0.20	3.0	2.0
0.10	4.5	2.5
0.05	8.0	3.5

Experiments indicating rapid ionophore dissociation and redistribution in red cells

Albumin has been shown to bind the ionophore A23187 with a high affinity [17]. Addition of a large albumin concentration 10 s before an excess of EGTA to a suspension of Ca-equilibrated cells containing enough ionophore to promote Ca release with a rate constant of 1.67 min^{-1} induces a 130-fold reduction in efflux rate (Fig. 3). The residual flux could be fitted by a single exponential to the origin, indicating that ionophore extraction had been completed within the 10-s interval.

Such rapid rates of onset and termination of ionophore-mediated Ca^{2+} fluxes as observed upon addition of ionophore [10] or albumin (Fig. 3) would predict rapid ionophore redistribution among cells, and this is shown in Fig. 4. Mixing equal volumes of Ca-equilibrated cell suspensions with very different original ionophore contents and Ca^{2+}-permeabilities resulted in Ca release upon EGTA addition which could be described by a single exponential rather than a composite of the original fast and slow components. The observed rate constant was 0.61 ± 0.02 min^{-1}. Assuming perfect redistribution of the ionophore contained in the original cell suspensions, and assuming that the ionophore-induced Ca^{2+}-permeability increases with cell ionophore content raised to the 1.5 power as previously reported [15,16], the calculated value was 0.71 min^{-1}. The small deviation between observed and calculated values may be caused by a slight ionophore-adsorption resulting from the mixing procedure.

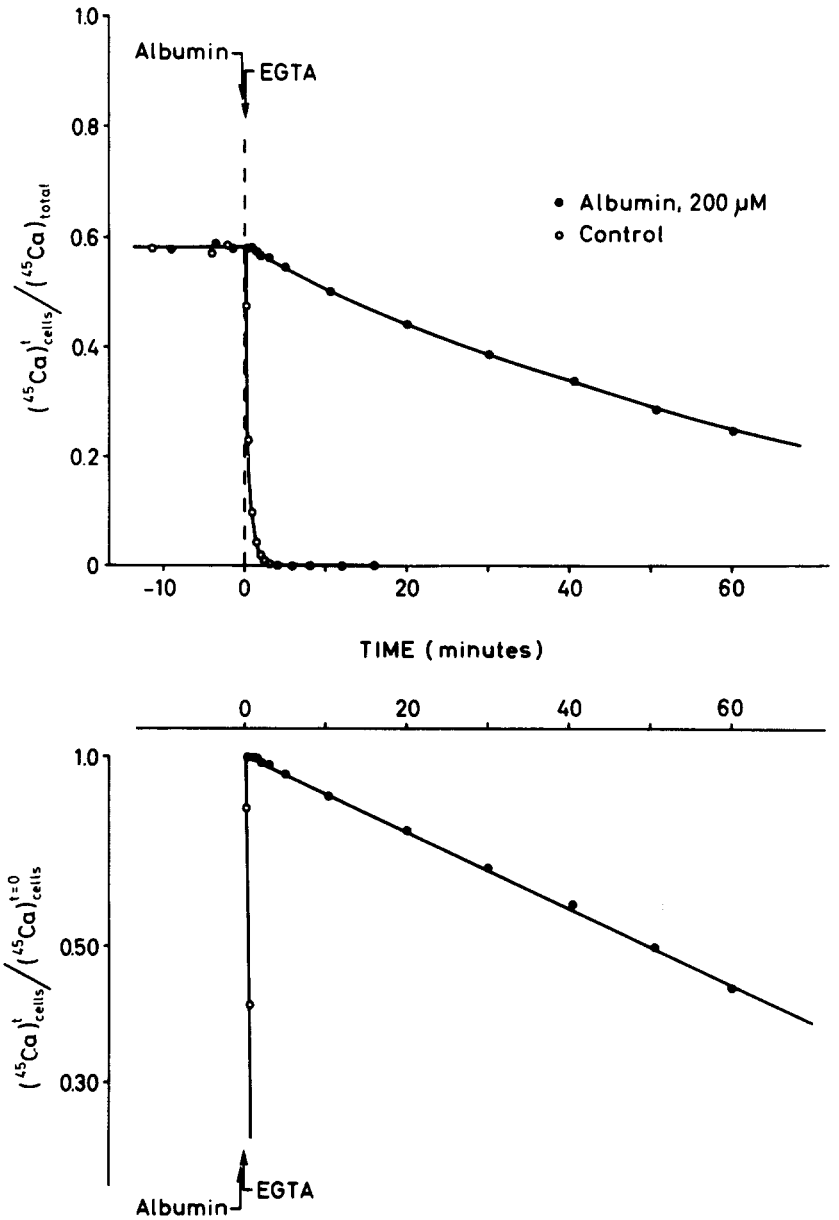

Fig. 3. Net Ca^{2+} efflux following addition of excess EGTA to Ca equilibrated cell suspensions in the presence of 2 μM ionophore A23187 (maximum likelihood estimate of rate constant $k = 1.67 \pm 0.04$ min^{-1}). In the upper curve 200 μM albumin (defatted) was added to the cell suspension 10 s before the start of efflux ($k = 0.0128 \pm 0.0014$ min^{-1}). Other experimental conditions as in Fig. 2.

Discussion

The results reported here demonstrate homogeneity of ionophore-induced Ca^{2+}-permeabilities in ATP-depleted red cells and indicate that the equilibrium distribution of the ionophore in the membrane is identical for all the cells. Direct measurements of ionophore content of the cells [15,16] has shown a partition ratio cell/medium of about 60, with about half of the cell-associated

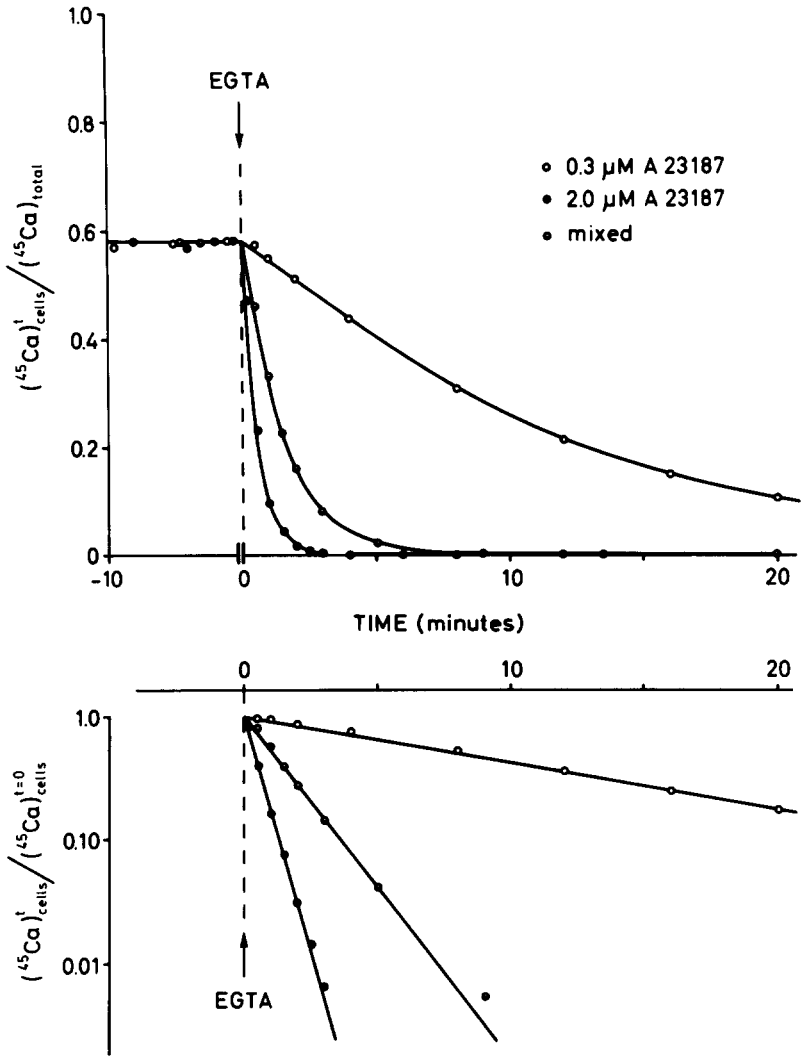

Fig. 4. Net Ca^{2+} efflux following addition of excess EGTA to Ca equilibrated cell suspensions with 0.3 and 2 μM ionophore A23187 (maximum likelihood estimate of rate constants: $k = 0.082 \pm 0.002$ min^{-1} and $k = 1.67 \pm 0.04$ min^{-1}, respectively). The middle curve reports net Ca efflux from a 1 : 1 mixture of the high- and low-ionophore cell suspensions. It should be noted that the efflux from the mixed cell suspension 5–10 min after mixing follows a single exponential (maximum likelihood estimate $k = 0.61 \pm 0.02$ min^{-1}). Other experimental conditions as in Fig. 2.

ionophore confined within the membrane. The present results suggest that at least the membrane-associated ionophore is in dynamic equilibrium with the ionophore in the medium, allowing rapid redistribution to occur upon ionophore addition or removal.

The 'voltage clamping' effect of the high-K^+ medium used in the present experiments would tend to generate a uniform membrane potential in all the cells under conditions of maximal activation of the Ca^{2+}-sensitive K^+-channel [5,9]. This means that the intracellular concentration of ionized Ca at equilibrium and therefore the unidirectional Ca^{2+} fluxes must have been almost identical for all the cells. If there had been cells with a higher total Ca content than others, i.e. with a higher Ca buffering capacity, they would have taken longer to equilibrate with ^{45}Ca at constant

flux or longer to release their Ca under conditions of net efflux, thus contributing slower components to the flux curves. The conspicuous absence of such components, therefore, demonstrates homogeneity of Ca content and cytoplasmic Ca buffering as well as of ionophore-induced Ca^{2+}-permeability among the cells. Whatever the relation between ionophoric effect and cell ionophore content, the factors that determine the equilibrium distribution of ionophoric units within the red cell membrane ought, therefore, to be similar in all cells, at least in ATP-depleted red cells.

If the ionophore A23187 induces an homogeneous increase in Ca^{2+}-permeability in fed red cells such as that demonstrated here for ATP-depleted cells, any ionophore-induced heterogeneity of Ca-content present in fed red cells must be caused by differences in Ca^{2+}-pumping resulting either from differences in metabolism or Ca^{2+}-pump-state in different cells.

If the mean cell Ca-content were concentrated in only 15% of the cells, as claimed by Hoffman et al. [12] in experiments meant to reproduce the low-ionophore (1 μM A23187) conditions of Lew and Ferreira [9], these cells would have to be near Ca equilibrium. Their pumps must, therefore, be unable to balance the ionophore-induced Ca^{2+} influx. All the other cells, with a similar Ca^{2+} influx (about 10 mmol/l cells h at an ionophore concentration of 1 μM, corresponding to a cell ionophore content of about 7 μmol/l cells, see Table I), would have to sustain near maximal Ca^{2+}-extrusion rates through their pumps while maintaining the intracellular Ca^{2+} levels below the activation threshold of a high Ca^{2+}-affinity K^+-channel. This would only be possible if the Ca^{2+}-affinity of the Ca^{2+}-pump were much higher than that of the K^+-channel. There are, however, enough uncertainties concerning V_{max} and $K_{1/2}$ of the Ca^{2+}-pump and K^+-channel in intact red cells to accommodate many hypotheses. Heterogeneity of Ca content, therefore, cannot be ruled out at present but participation of Ca^{2+} permeability and cytoplasmic Ca-buffering in it is most unlikely.

There is not enough information available to carry out a critical analysis of the alternative interpretations compatible with the results of Hoffman et al. [12]. Differences in Ca^{2+}-sensitivities of the K^+-channel [9,10] would, however, seem difficult to exclude whether or not Ca^{2+}-pump-induced heterogeneities in the Ca content of fed cells occur at low ionophore concentrations.

Acknowledgements

We wish to thank David Knight and R.M. Bookchin for useful discussions, Jackie Gray and Inga Somer for excellent technical assistance and the MRC (U.K.) and Carlsberg Foundation (Denmark) for funds.

References

1 Reed, P.W. and Lardy, H.A. (1972) J. Biol. Chem. 247, 6970–6977
2 Pressman, B.C. (1976) Annu. Rev. Biochem. 45, 501–530
3 Ferreira, H.G. and Lew, V.L. (1976) Nature (London) 259, 47–49
4 Flatman, P. and Lew, V.L. (1977) Nature (London) 267, 360–362
5 Lew, V.L. and Brown, A.M. (1979) in Detection and Measurement of Free Ca^{2+} in Cells (Ashley, C.C. and Campbell, A.K., eds.), pp. 423–432, Elsevier, North-Holland, Amsterdam
6 Brown, A.M. (1979) Biochim. Biophys. Acta 554, 195–203
7 Flatman, P.W. and Lew, V.L. (1980) J. Physiol. (London) 305, 13–30
8 Flatman, P.W. (1980) J. Physiol. (London) 300, 19–30
9 Lew, V.L. and Ferreira, H.G. (1976) Nature (London) 263, 336–338
10 Lew, V.L. and Ferreira, H.G. (1978) in Current Topics in Membranes and Transport (Kleinzeller, A. and Bronner, F., eds.), Vol. 10, pp. 217–277, Academic Press, New York
11 Sarkadi, B., Szász, I. and Gárdos, G. (1976) J. Membrane Biol. 26, 357–370
12 Hoffman, J.F., Yingst, D.R., Goldinger, J.M., Blum, R.M. and Knauf, P.A. (1980) in Membrane Transport in Erythrocytes, Alfred Benzon Symposium 14 (Lassen, U.V., Ussing, H.H. and Wieth, J.O., eds.), pp. 178–195, Munksgaard, Copenhagen
13 Lew, V.L. and Simonsen, L.O. (1981) J. Physiol. (London) 316, 6–7P
14 Lew, V.L. (1971) Biochim. Biophys. Acta 233, 827–830
15 Simonsen, L.O. and Lew, V.L. (1980) in Membrane Transport in Erythrocytes, Alfred Benzon Symposium 14 (Lassen, U.V., Ussing, H.H. and Wieth, J.O., eds.), pp. 208–212, Munksgaard, Copenhagen
16 Lew, V.L. and Simonsen, L.O. (1980) J. Physiol. (London) 308, 60P
17 Simonsen, L.O. (1981) J. Physiol. (London) 313, 34–35P
18 Harrison, D.G. and Long, C. (1968) J. Physiol. (London) 199, 367–381
19 Bookchin, R.M. and Lew, V.L. (1980) Nature (London) 284, 561–563
20 Ross, G.J.S. (1980) MLP, Maximum Likelihood Program, Rothamsted Experimental Station, Harpenden, Hertfordshire, U.K.
21 Canham, P.B. and Burton, A.C. (1968) Circ. Res. 22, 405–422